Arch. Mech., 50, 1, pp. 691–701, Warszawa 1998
FIFTY YEARS OF THE ARCHIVES OF MECHANICS

# Effect of miss-distance on the airfoil-vortex interaction Experiment

W. SELEROWICZ, G. SOBIERAJ, A. SZUMOWSKI
and J. PIECHNA (WARSZAWA)

THE EFFECT of a strong vortex interacting with an airfoil flow is investigated experimentally by means of a shock tube. The experiments follow the previous theoretical work [11] on this subject. The instantaneous pressure distributions and histories of lift coefficient during the vortex passage are presented. The flow is visualised using the schlieren method. It is found that due to the viscosity of the air not taken into account in numerical study, the effect of miss-distance in the range of up to 0.5 chord length is weaker than it was initially predicted.

## 1. Introduction

A TIP VORTEX shed from the helicopter rotor blade can interact with the following blade. This happens during the helicopter descent with a deep turn and its low-powered approach to landing. The strongest interaction occurs when the vortex filament passes parallel at a small distance from the blade plane. A specific case of this type of interaction shows the head-on impact of the vortex core on the leading edge.

The parallel airfoil-vortex interaction (AVI) was investigated by many authors. Both the numerical and the experimental methods were used. Considering a wide range of the flow Mach number which can exist during the helicopter blade rotation, the incompressible and compressible (also transonic) flows were studied. In the experiments the vortex needed for interaction was produced by a preceding pitched airfoil singly [1] or continuously in wind [2] or water [3] tunnels. The wind tunnel experiments, however, do not provide strong vortices and hence do not allow one to obtain sufficiently strong effects of the vortex interaction. This especially concerns the acoustic effects. For a weak vortex, the sound pressure produced during the interaction appears to be of the order of magnitude of the background disturbances. This disadvantage can be partly avoided by using starting vortex of a lifting airfoil placed in a shock tube. This technique was used by LENT *et al.* [4], LEE and BESHADER [5] and KAMIŃSKI and SZUMOWSKI [6]. By applying the interferometric [4, 5] and schlieren method [6] for flow visualisation, they observed an acoustic wave generated during the head-on collision.

Majority of the papers on the AVI phenomenon consider the acoustic effects, but only a few of them deal with the loading. References [1, 2, 7, 8] present

variation of the loading for very low flow velocities. Even in this case considerable changes of the airfoil surface pressure and the lift coefficient have been observed. For the transonic flow range [9, 10] these changes are additionally strengthened due to the shock waves which move along the airfoil surfaces (suction and pressure surfaces) during the interaction.

The parallel airfoil-vortex interaction is controlled, first of all, by the following parameters:

(i) the miss-distance which is defined as a distance measured at infinity between the vortex trajectory and the stream line passing through the stagnation point;

(ii) radius of the vortex core ($r_0$),

(iii) circulation ($\Gamma_0$) at $r = r_0$, and

(iv) flow Mach number at infinity.

The present experimental work concerns the effect of the first of four parameters mentioned above. It follows the previous numerical study [11] in which the airfoil flow was computed by means of the Euler solver. This paper, like [11], is focussed on aerodynamic effects: surface pressure and loading variations during the interaction.

The experiments conducted in this work correspond to the calculation results presented in Ref. [11]. However, the period of time in which the pressure histories during the interaction were possible to be measured, was much longer than the period available in computation. This was due to the relatively large length of the shock tube which enabled the authors to have a steady background flow (not disturbed by the waves reflected at closed ends of the shock tube or by the entropy discontinuity surface) for a relatively long time.

## 2. Experimental facility

The experiments were conducted in a conventional two-chamber shock tube of dimensions shown in Fig. 1. The rectangular cross-section of the tube was modified by mounting the triangular slots along the top and bottom walls to conceal the oblique waves which appear during the shock wave-airfoil interaction. Each experiment was prepared by evacuating the air from the low pressure chamber to obtain a vacuum up to 8 kPa of absolute pressure. In the high pressure chamber the atmospheric pressure was maintained. The two NACA 0012 airfoils of chord length $c = 120$ mm were placed at a distance of 530 mm in the shock tube. The preceding airfoil was used to generate the vortex, and the following one to induce the AVI process. The former could be displaced across the shock tube to adjust the vortex trajectory. A constant angle of attack equal to 20° of this airfoil was maintained. The instantaneous pressure was measured by means of miniature Kulite pressure transducers distributed at the side wall

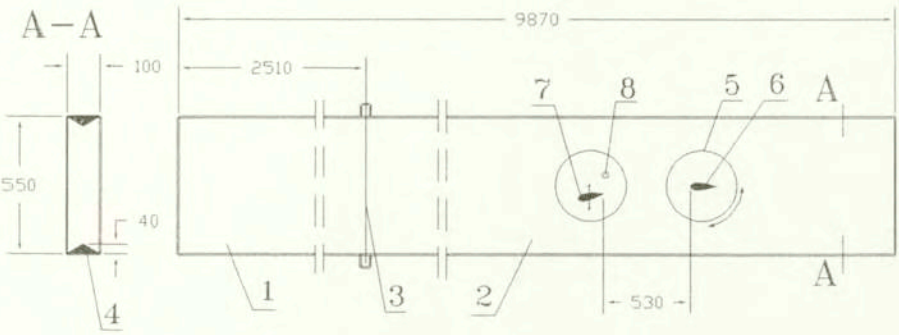


FIG. 1. Shock tube: *1* – high pressure chamber, *2* – low pressure chamber, *3* – diaphragm, *4* – slot, *5* – test section window, *6* – test airfoil, *7* – vortex generator, *8* – triggering transducer.

of the tube along the airfoil contour (Fig. 2). It was believed that due to their small diameters (2.3 mm), the measured pressure was equal to the actual airfoil surface pressure. This supposition was checked by comparing the measured wall pressure with the computed (Euler solver) airfoil surface pressure for the flow without the vortex (the vortex generator was removed during this experiment). The results are shown in Fig. 3. Good agreement between the corresponding pressure histories in each point except one (at the leading edge) can be noted. The discrepancy between the measured wall pressure and the calculated surface pressure at $x/c = 0$ appears to be caused by the nonuniform pressure distribution is the region close to the stagnation point (the transducer shows average pressure on its face).

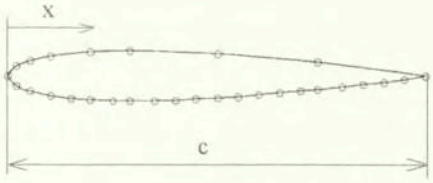


FIG. 2. Distribution of pressure transducers.

The vortex trajectory was identified by measuring the pressure histories at ten points densely distributed along the line normal to the airfoil plane, one chord upstream the airfoil.

The flow was visualised by means of the schlieren method. The Cranz-Schardin system which allows one to have 8 consecutive photographs during one experiment was used.

The experiments were performed with a constant flow Mach number $M_1 = 0.69$ which in this case corresponds to the following values of the flow velocity,

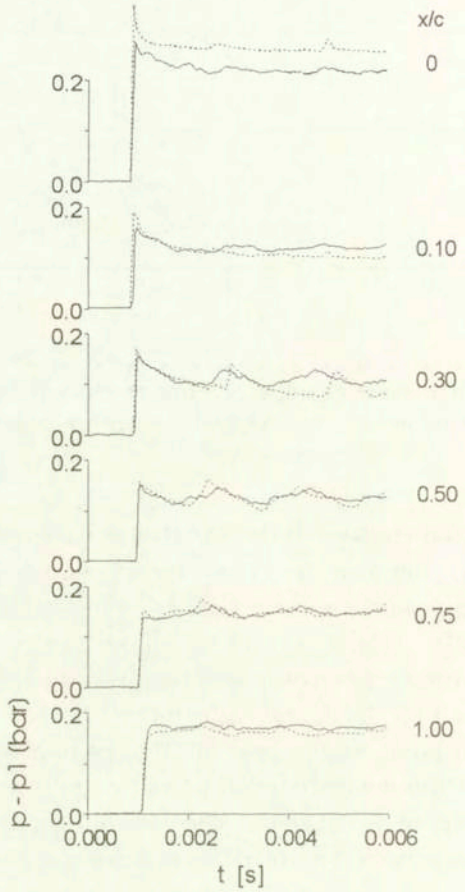


FIG. 3. Wall pressures (continous lines) measured at selected points (see Fig. 2) and the corresponding calculated airfoil surface pressures (dashed lines). Flow without a vortex.

the speed of sound and pressure, respectively: $u_1 = 276$ m/s, $a_1 = 400$ m/s and $p_1 = 22.6$ kPa. The vortex properties were as follows: relative radius of the vortex core $r_0/c = 0.045$, maximum circulation (at $r_0$) 50 m$^2$/s. Decay coefficient of velocity in the vortex $\alpha = 0.15$ (see [12]).

## 3. Results

The starting vortex shed from the airfoil (vortex generator) at 20 deg. angle of attack is followed by a wide vortex path. This causes that the flow at the test airfoil when it is reached by the vortex path, becomes strongly turbulent. The vortex path, however, forms with some delay after the starting vortex leaves the test airfoil and actually does not affect the AVI process. This can be seen in Fig. 4 which shows the wall pressure histories measured at two points

($x/\ c = 0.05$ and 0.5) in the upper and bottom contours of the airfoil, for identical experimental conditions. It can be observed that the random disturbances due to the vortex path are insignificant in the initial period (up to 3 ms after the shock wave passage) of the presented pressure histories. This period is nearly ten times longer than the time of the vortex passage along the airfoil. Nevertheless, the experiments were repeated a few times for each miss-distance considered to avoid random effects during the interaction. Then the average histories of the wall pressure measured at selected points in the airfoil contour were determined. They are presented below.

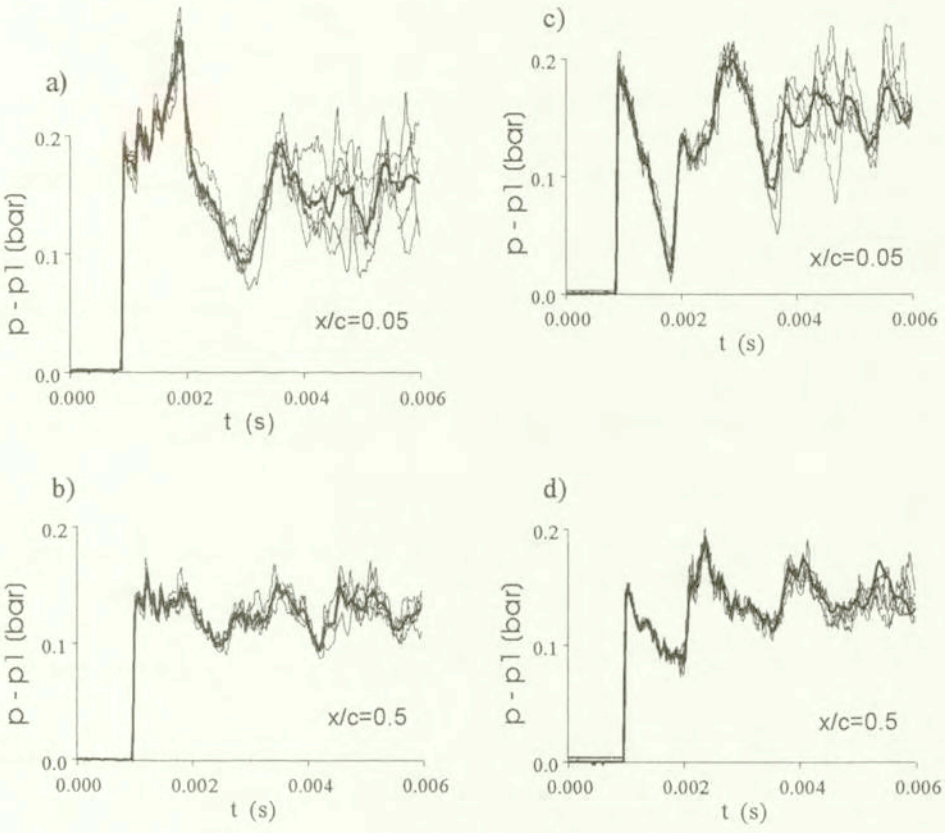


FIG. 4. Histories of wall pressure at two point in the bottom (a,c) and upper (b,d) airfoil contour (see Fig. 2) obtained for five identical experiments. Thick line – average of five histories.

In Fig. 5 the wall pressure signals for transducers symmetrically distributed along the upper and the bottom airfoil contour are presented. One can see that the pressure considerably varies during the interaction. This concerns, first of all, the leading section of the airfoil. Initially the pressure increases at the upper surface ($p_u$) and decreases at the bottom one ($p_b$). It is due to the stagnation

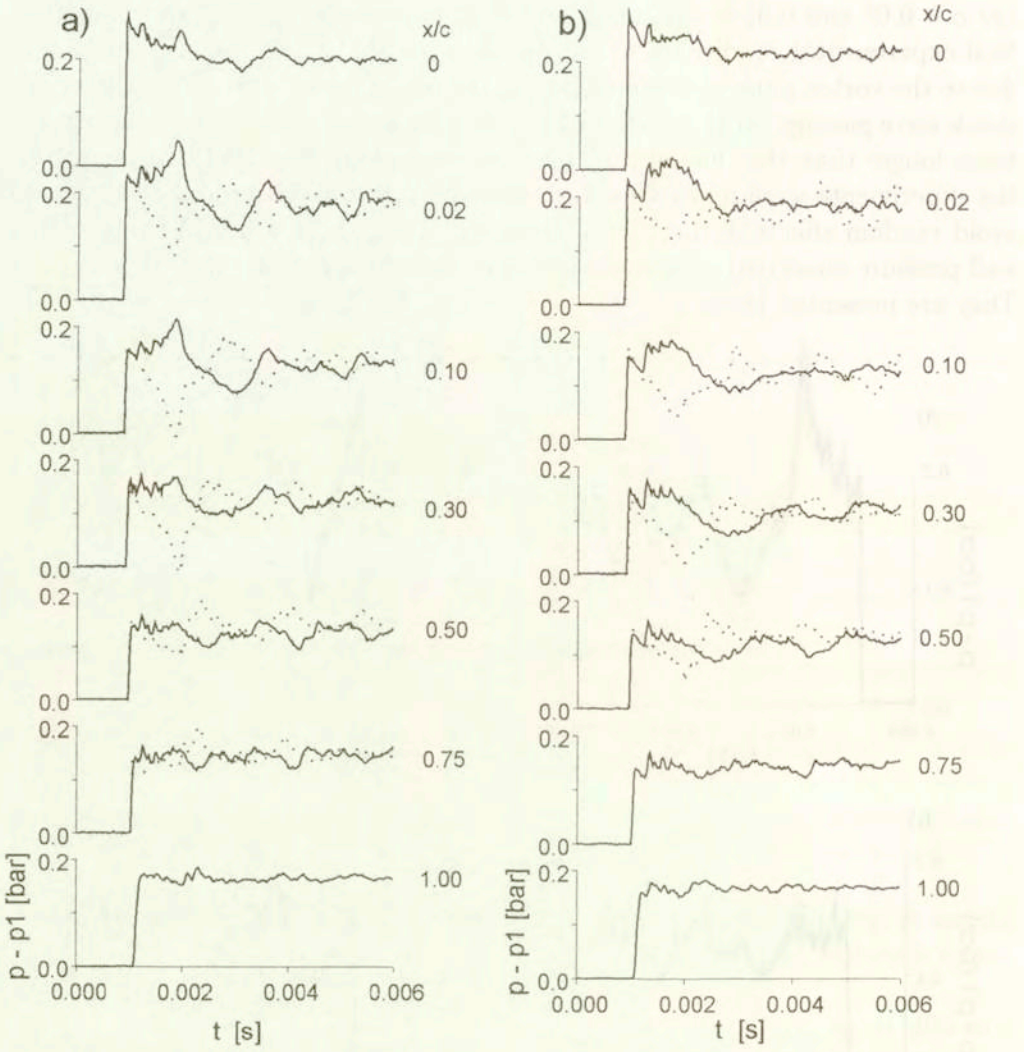


FIG. 5. Wall pressure histories for the upper (continuous lines) and bottom (dotted lines) airfoil contour.

point displacement on the upper surface when the clockwise rotating vortex approaches the airfoil. After some delay, when the stagnation point comes back to its previous position, $p_u$ decreases and $p_b$ increases. The pressure oscillations which are induced in this way exist for a relatively long time after the vortex leaves the airfoil. This effect was also observed by KAMIŃSKI and SZUMOWSKI [6]. The strongest pressure variations in the present experiments were noted at the point $x/c = 0.05$ at the bottom contour of the airfoil (Fig. 2). The pressure histories at that point are shown in Fig. 6 for several values of miss-distance. It is visible that the pressure decreases with nearly the same rate for all miss-distances considered

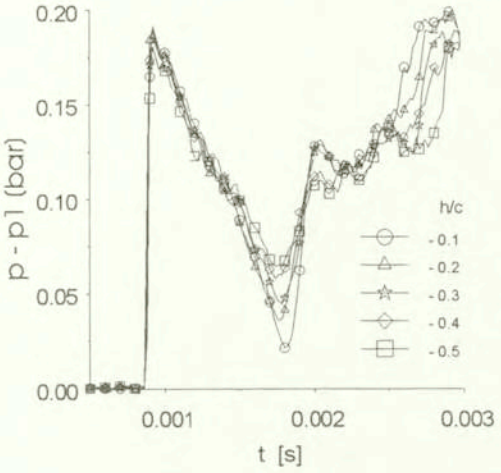


FIG. 6. Histories of wall pressure at $x/c = 0.0$ (bottom contour) for various miss--distances.

when the vortex approaches the airfoil. For small miss-distances, however, the pressure reaches a lower minimum.

Instantaneous pressure distributions along the chord for extreme values of miss-distance considered are shown in Fig. 7 (they are compared with the pressure distributions for steady flow without the vortex). One can observe an increasing pressure difference between the bottom and the upper surface during the initial phase of interaction (Fig. 7a, b and 7g, h). As a result, the lift coefficient decreases (Fig. 8) and reaches negative values. In the following phase of interaction the lift coefficient grows due to increasing bottom surface pressure and decreasing upper surface pressure (Fig. 7c and 7i). After some delay it reaches a maximum and decreases again. The measured lift coefficient histories shown in Fig. 8 are compared with the calculated ones for $x/c = -0.1$ obtained in [11]. Qualitative agreement between the corresponding curves can be noted. However, the rate of changes of $c_l$ predicted by theory is about twice as large as the measured one.

The following explanation of this discrepancy can be proposed. The time required by the vortex to travel along the airfoil is about 0.4 ms (see data given in the second section). This time is represented in Fig. 8 by the section of abscissa which follows the minimum of the curve $c_l(t)$. During this interval (and also the preceding one) it was predicted [11] that the vortex maintains its coherent structure. Taking into account this feature one can suppose that the steep increase of $c_l$ predicted in calculations appears to be a direct effect of the vortex travelling along the airfoil.

The calculations presented in Ref. [11] were performed for inviscid gas. However, due to the viscosity of the real air and the presence of shock waves with

complicated structure, the flow velocity induced by the vortex in the vicinity of the air surface is strongly disturbed.

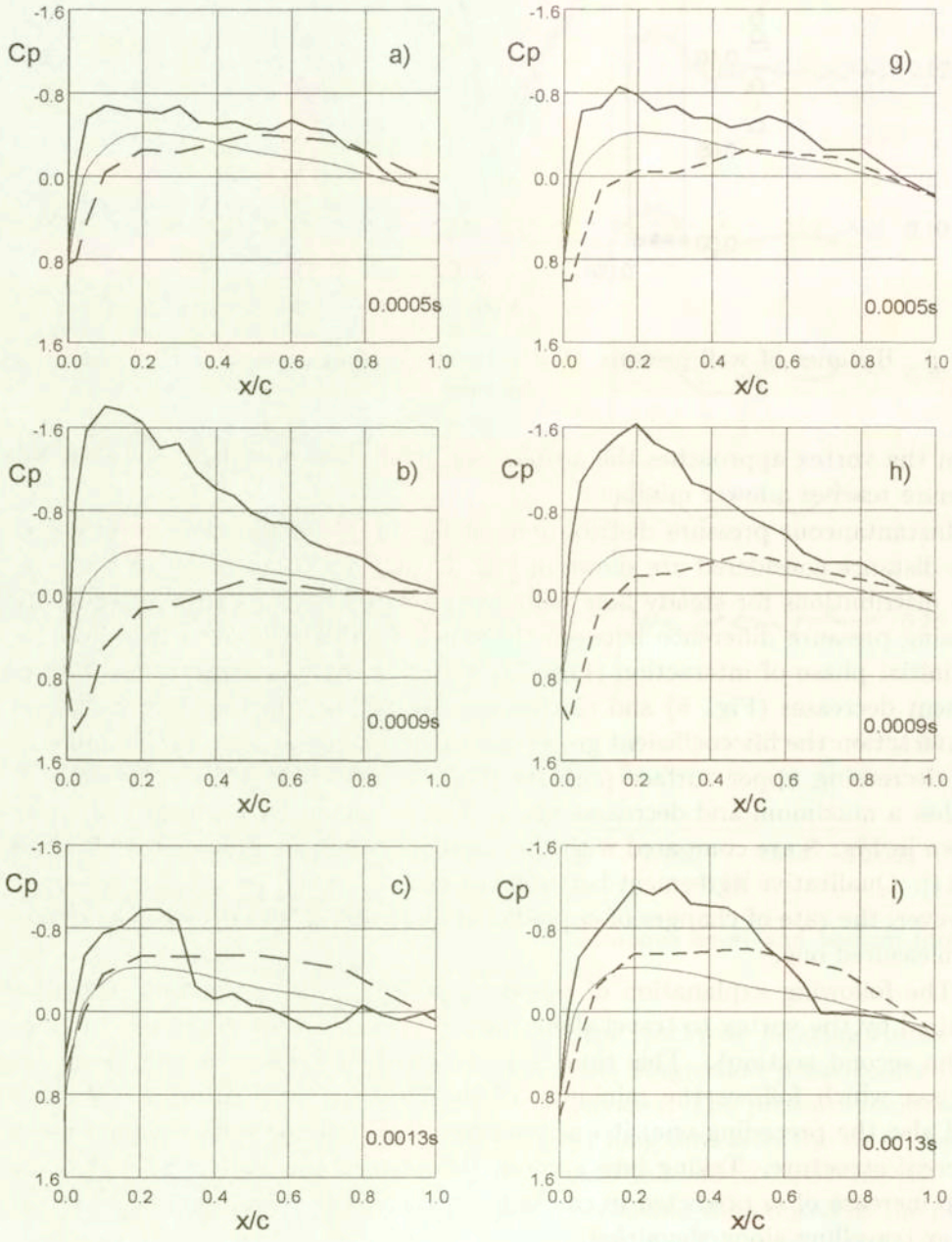


[FIG. 7.]

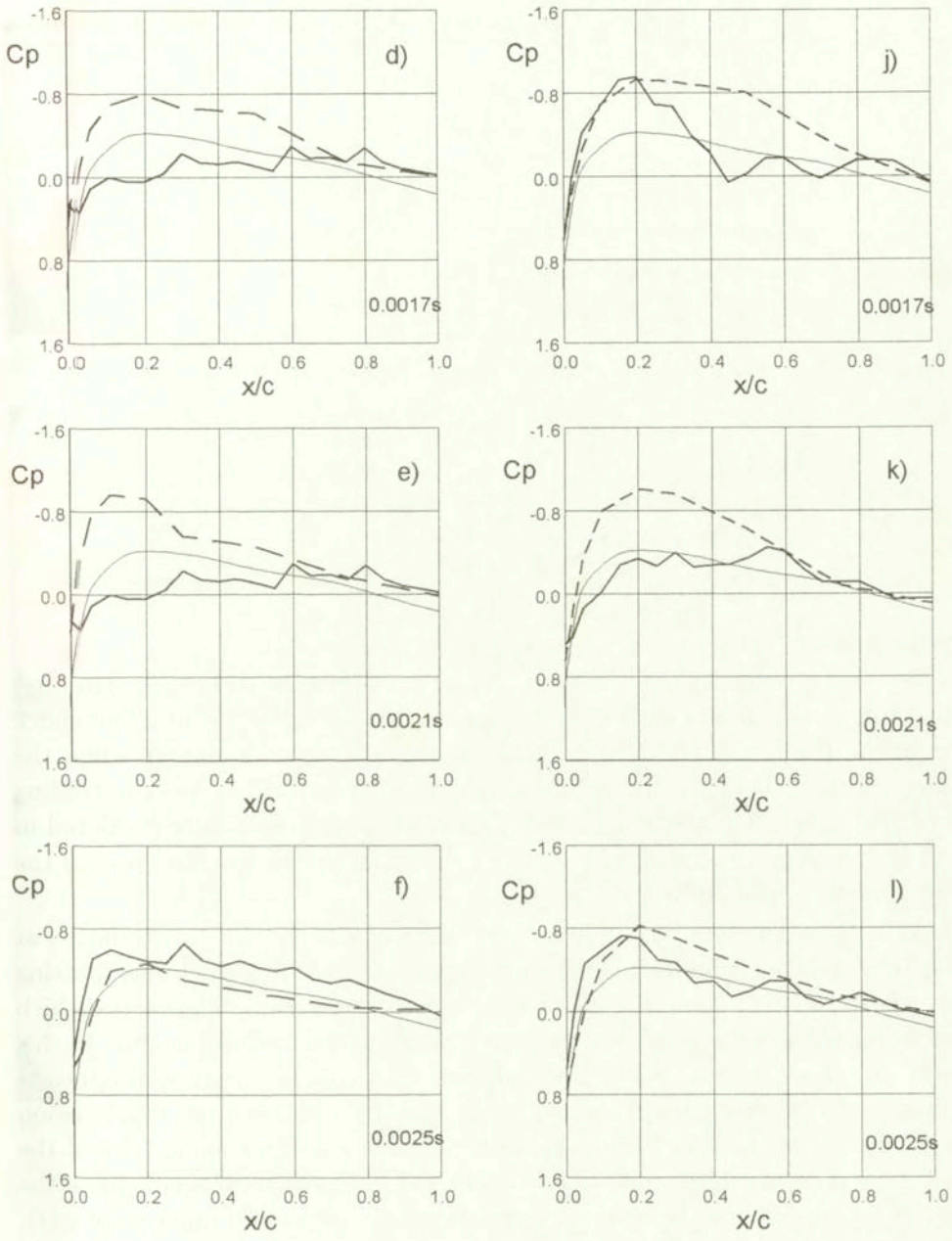


FIG. 7. Steady (thin continuous line) and instantaneous (thick continuous and dashed lines) presure distributions for $h/c = -0.1$ (first column) and $h/c = -0.5$ (second column) along upper (continuous) and bottom (dashed) airfoil contour.

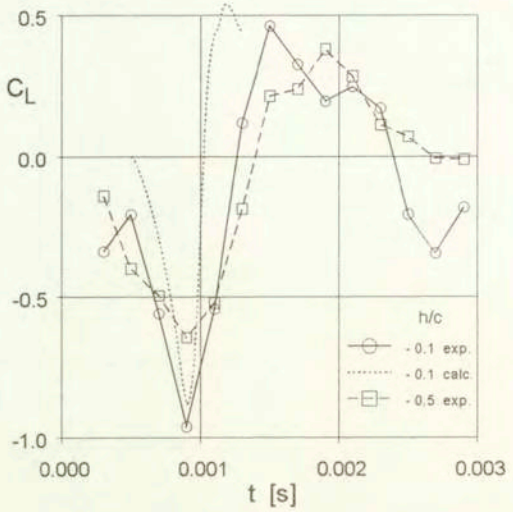


FIG. 8. Histories of a lift coefficient.

This can be noted in the schlieren photographs present in Fig. 9. The first photograph in this figure shows the vortex approaching the airfoil. The shock waves on both sides of the airfoil visible in this photograph emerge when the incident shock (generated due to the diaphragm break-up) reaches the trailing edge of the airfoil. These shocks which move slowly upstream were predicted in [11]. The following photographs (b and c) show the vortex when it reaches the leading section of the airfoil.

In this phase the "lambda" – like shock wave of a long stem can be noted at the bottom surface. It limits a supersonic region induced by a clockwise rotating vortex. Both the vortex and the shock wave move downstream. The vortex which moves faster reaches the shock wave approximately at a half-chord length. In this moment the flow pattern drastically changes. The coherent vortex disappears. Simultaneously, the separation bubble which initially existed in the shock region (along the stem of the shock wave) spreads out as far as the trailing edge of the airfoil. This process which could not be predicted for inviscid air seems to be the reason of the discrepancy between the calculated and measured function of $c_l(t)$.

## 4. Concluding remarks

The effect of miss-distance (in the range considered) on the airfoil flow is weaker than it was predicted in a previous numerical study [11]. This is due to the turbulent viscous stresses which are considerably influenced by the passing vortex, even for relatively large $h/c$. The vortex induces flow oscillations which exist for a long time after the vortex leaves the airfoil flow region.

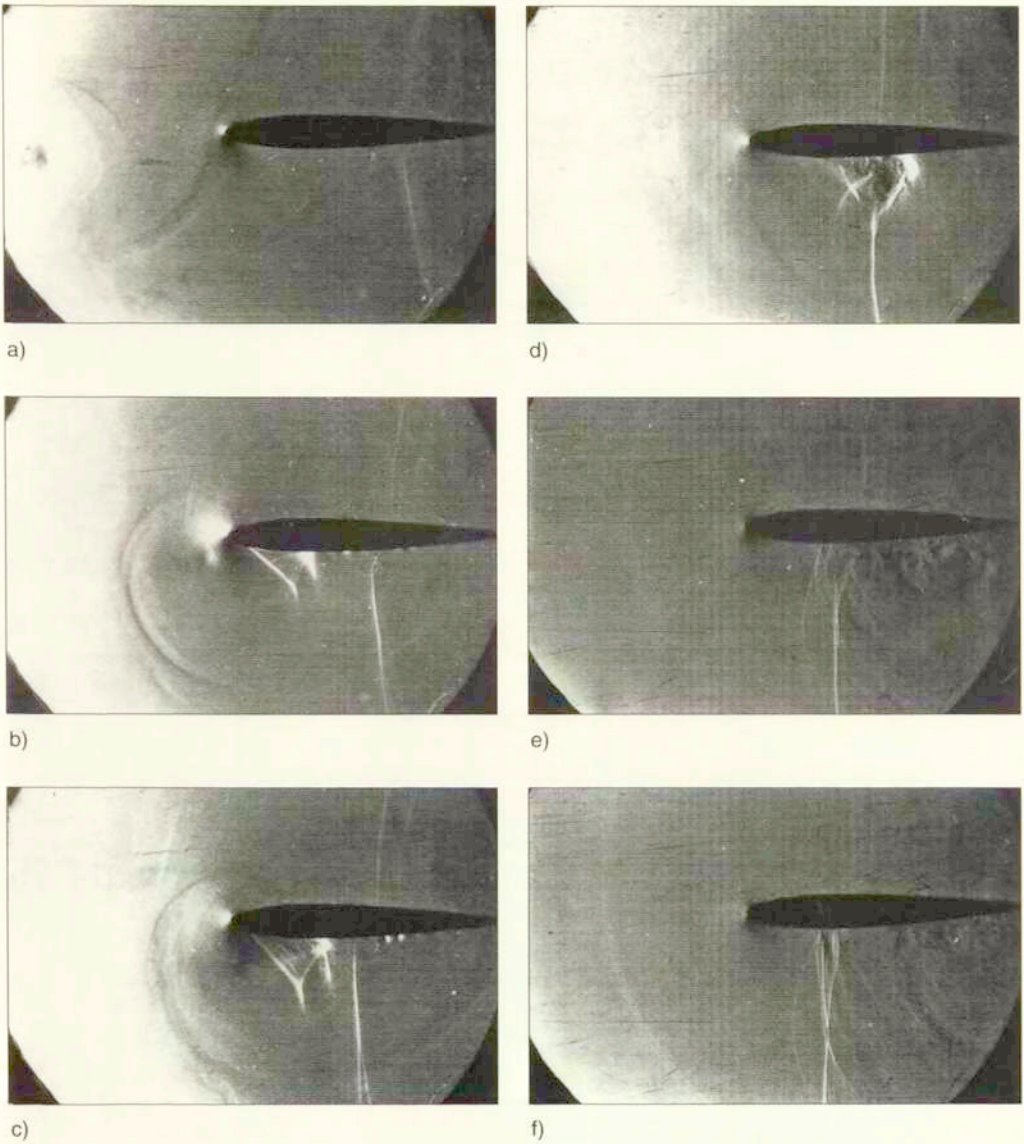


FIG. 9. Photographs of the flow during the AV1. Time interval between photographs (a) and (b) – 0.2 ms, for the following photos – 0.1 ms.